Supplementary data

Hydrothermal Enhanced Etching of Ni for Directly Recovery of Gold Flakes from Electronic Waste

Shuling Shen[a*], Yu Chu[a], Ziwei Feng[a], Zheng Du[a], Huixin Xiu[a], Xinjuan Liu[a], Shuning Xiao[a], Zhihong Tang[a], Jing Li[a], Xun Wang[b*]

[a]School of Materials and Chemistry, University of Shanghai for Science and Technology, Shanghai, 200093, P. R. China

[b]Key Lab of Organic Optoelectronics and Molecular Engineering, Department of Chemistry, Tsinghua University, Beijing, 100084, P. R. Chin

*Corresponding authors: slshen@usst.edu.cn; wangxun@mail.tsinghua.edu.cn

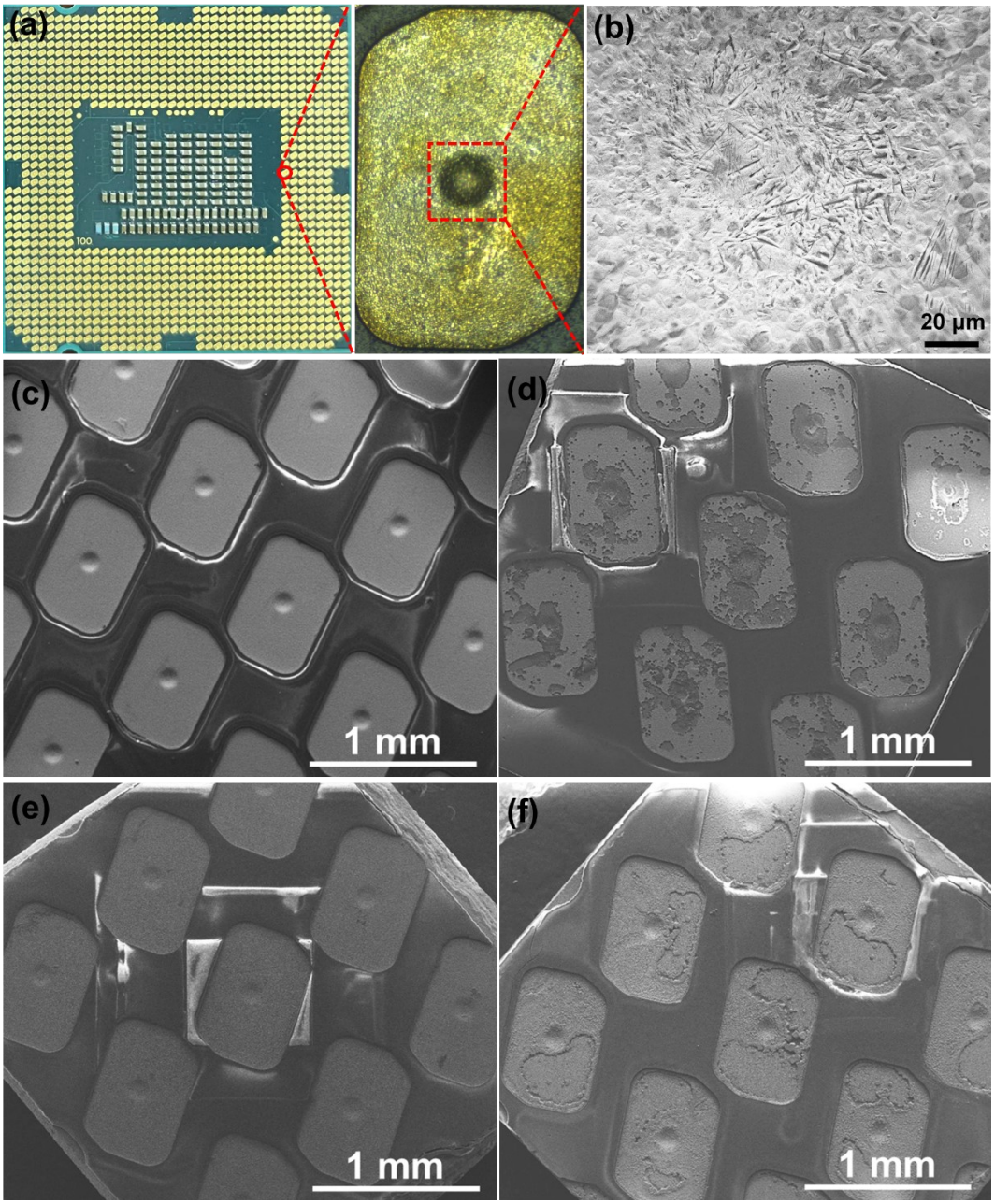

Figure S1 (a) Photo of a waste CPU and a typical contact on the CPU. (b) SEM image of the center of a typical contact. SEM images of the waste CPU board after different hydrothermal reaction time: (c) 0 h, (d) 6 h, (e) 12 h and (f) 36 h.

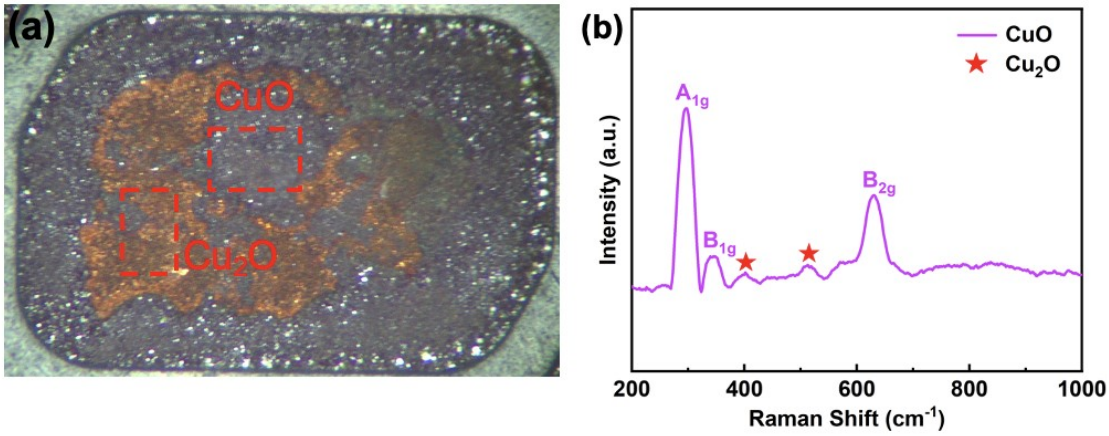

Figure S2 (a) Optical microscope photo and (b) Raman spectra of a typical contact on the waste CPU after 36 h of hydrothermal reaction.

Table S1 Sample XPS binding energy positions and corresponding species.

Sample	Elemental	Binding energy (eV)	Species
Before	Au	83.9	Au^0
	Ni	852.1	Ni^0
		855.5	NiO
	Cu	932.4	Cu and Cu_2O
		933.2	CuO
	O	529.7	CuO and NiO
		530.5	Cu_2O
		531.8	OH
After	Au	____	____
	Ni	____	____
	Cu	932.4	Cu and Cu_2O
		933.2	CuO
	O	934.7	$Cu(OH)_2$
		529.7	CuO
		530.5	Cu_2O
		531.8	OH
TiO_2-6	Ti	458.4	Ti^{4+} in TiO_2
	Ni	855.6	$Ni(OH)_2$
	O	529.6	TiO_2
		531.3	$Ni(OH)_2$ and OH

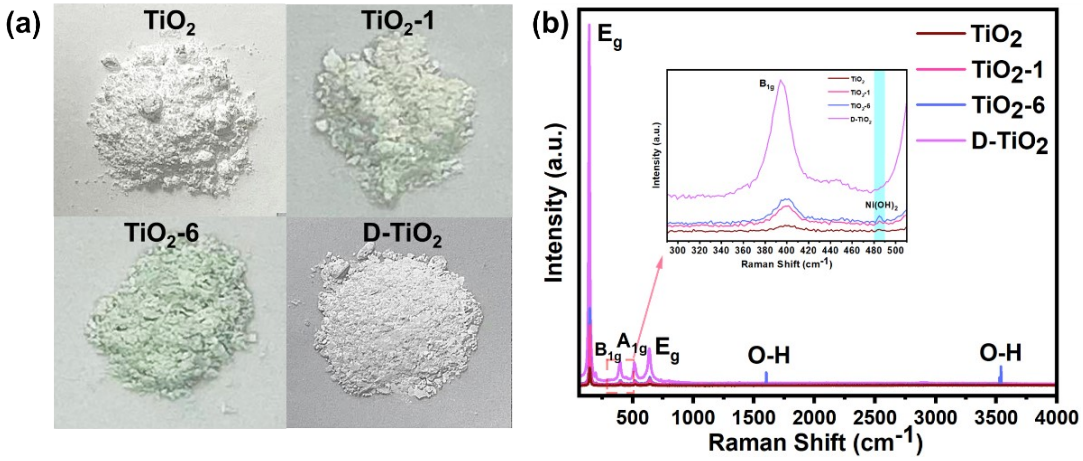

Figure S3 Optical photos and Raman spectra of TiO_2, TiO_2-1, TiO_2-6, and D-TiO_2.

The anatase TiO_2 displays characteristic peaks at 144 cm^{-1}, 395 cm^{-1}, 512 cm^{-1}, and 631 cm^{-1}, attributed to the Eg, B_{1g}, A_{1g}, and Eg Raman vibrations, respectively. Notably, there are no discernible Raman vibration peaks for rutile phase TiO_2 at 442 cm^{-1}. In the Raman spectra of TiO_2, intriguingly, with an increased cycle number, new characteristic peaks at 487 cm^{-1}, 1620 cm^{-1}, and 3647 cm^{-1} emerge in the TiO_2-6 sample. These peaks arise from the Ni-O vibration and O-H stretching vibration of $Ni(OH)_2$, which accumulates on TiO_2 as the cycle number increases. The vibrational peaks associated with Ni-O bonds and O-H stretching in $Ni(OH)_2$ were significantly attenuated in the decontaminated D-TiO_2 samples.

Table S2 The recovery rates of Au at different conditions.

Reaction time (h)	Reaction temperature (℃)	Catalyst dosage (mg)	The recovery rates of Au （%）
6	130	200	62.9
12	130	200	96.5
24	130	200	98.8
36	130	200	99.2
36	50	200	79.4
36	80	200	89.9
36	100	200	98.7
36	130	200	99.2
36	130	0	0
36	130	10	49.5
36	130	50	84.5
36	130	200	99.2

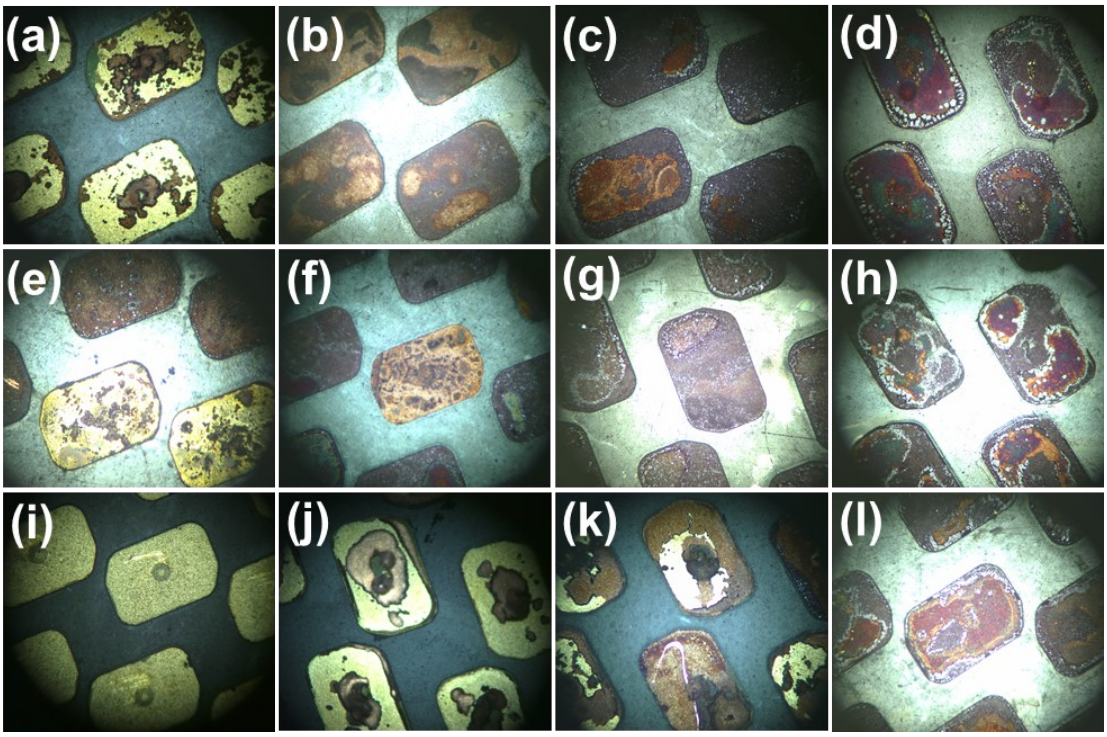

Figure S4 Optical microscope photos of CPU boards after hydrothermal reaction under different conditions. Reaction time: (a) 6 h, (b) 12 h, (c) 24 h, (d) 36 h. Reaction temperature: (e) 50 ºC, (f) 80 ºC, (g) 100 ºC, (h) 130 ºC. Dosage of catalysts: (i) 0 mg, (j) 10 mg, (k) 50 mg, (l) 200 mg.

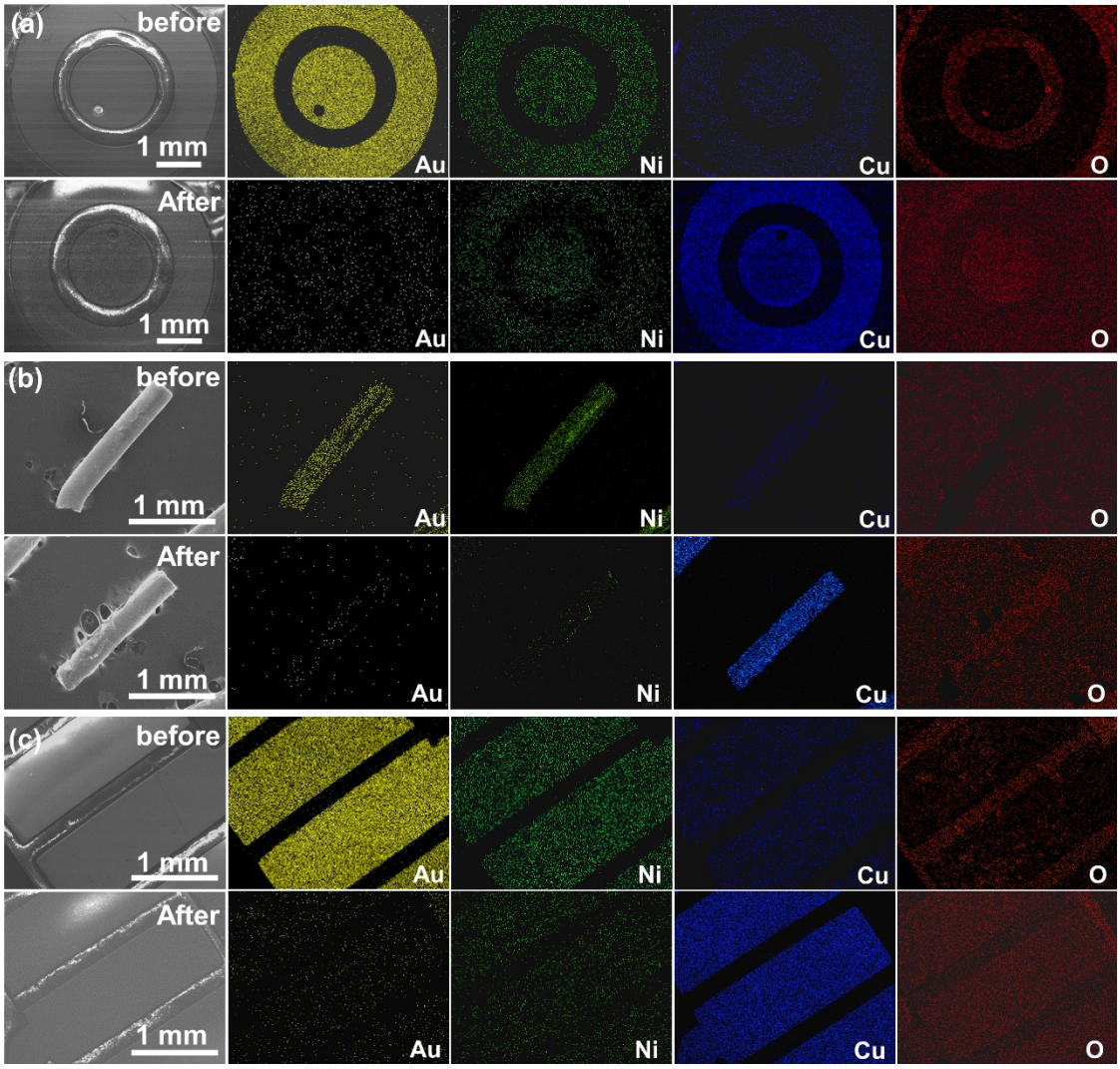

Figure S5 SEM images and Au, Ni, Cu and O elemental mapping images of different PCBs before and after hydrothermal reaction. (a) keypad PCB of a classic mobile phone, (b) pins from pin-type CPU and (c) computer memory stick.

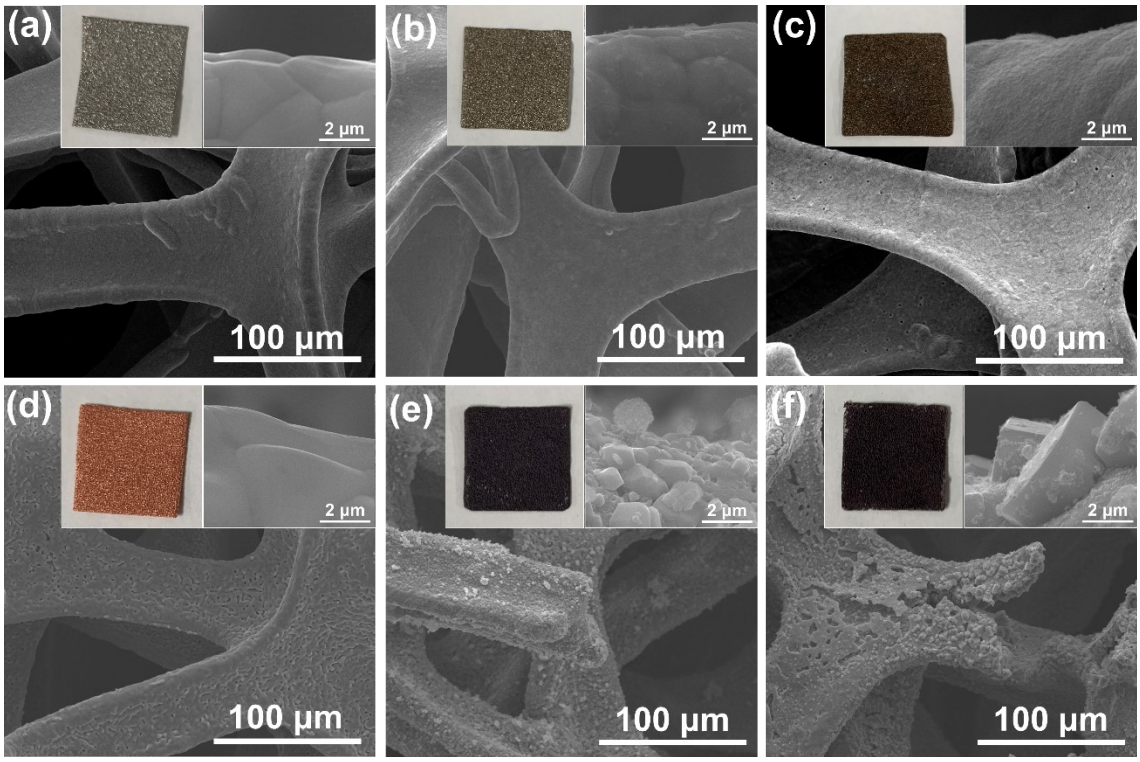

Figure S6 Photograph and SEM images of pure Ni foam: (a) before treatment, (b) after hydrothermal treatment without the catalyst, and (c) after hydrothermal treatment with the catalyst. Photograph and SEM images of pure Cu foam: (a) before treatment, (b) after hydrothermal treatment without the catalyst, and (c) after hydrothermal treatment with the catalyst.

Table S3 Atomic percentage of oxygen in Ni foam and Cu foam after hydrothermal treatment with and without the catalyst.

Sample	At %	Before treatment	Without the catalyst	With the catalyst
Ni foam	O	2.44	10.22	12.17
	Ni	97.56	89.78	87.83
Cu foam	O	3.61	15.62	27.47
	Cu	96.39	84.38	72.53

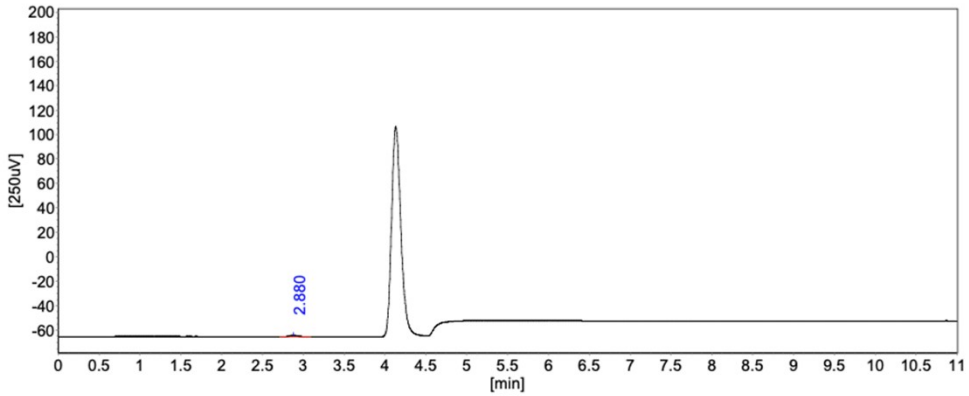

Analysis Results

Peak number	Composition	Residence time [min]	Peak height [250uV]	Peak area [250uV*s]	Area Ration %	Content [ppm]	Peak pattern
1	H_2	2.880	1.27	8.9	88.1339	131.4482	+BB
2		25.447	0.1	1.2	11.8661	0.000	BB
Total			**1.37**	**10.10**	**100.0000**	**131.4482**	

Figure S7 Gases in the autoclave after hydrothermal reaction.

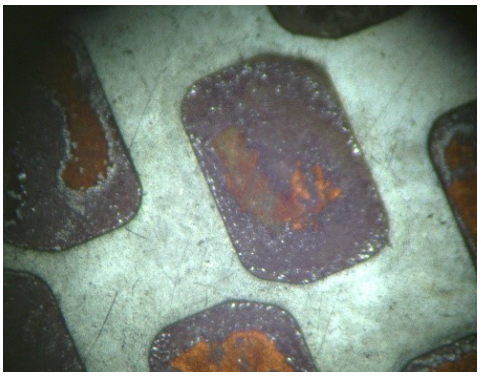

Figure S8 Optical microscope photo of CPU board after hydrothermal reaction without O_2 in the reaction system.

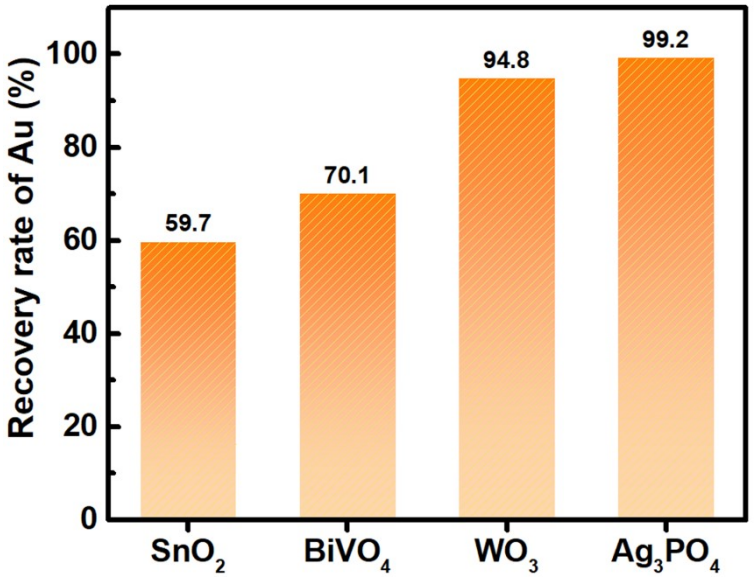

Figure S9 The recovery rate of Au with different catalysts.

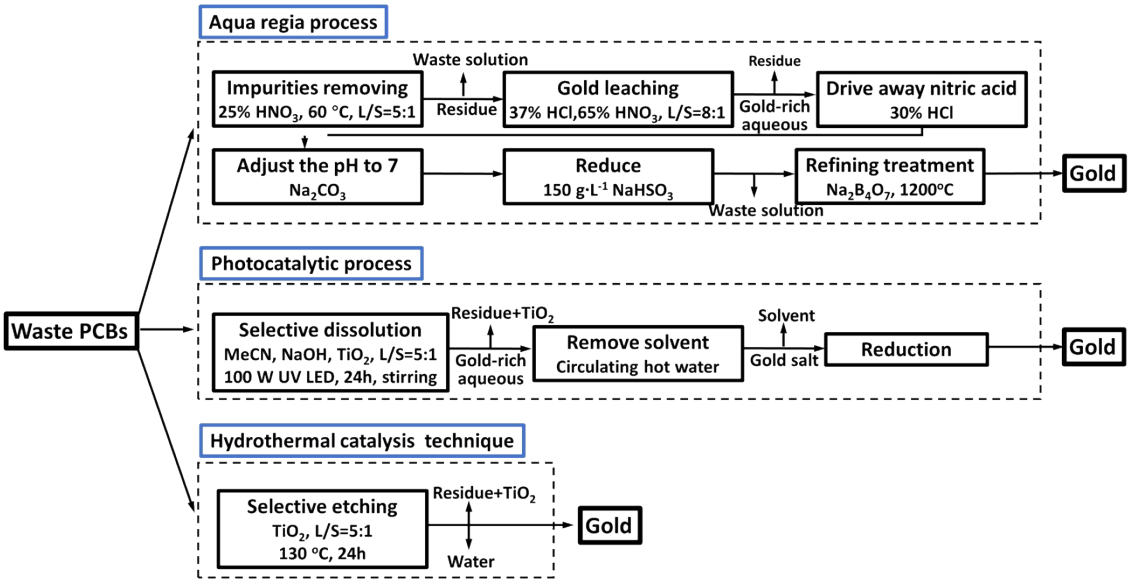

Figure S10 Comparation of hydrothermal catalysis technique with other methods for Au recovery from waste PCBs.

Table S4 The cost of recovering Au using aqua regia process (ref 1-3), photocatalytic process (ref 3-4) and our hydrothermal catalysis technique.

Method	Item	Unit price	Units	Total cost /Value ($)
Aqua regia process	Nitric acid	60.17	$\$\cdot L^{-1}$	395.99
	Hydrochloric acid	6.94	$\$\cdot L^{-1}$	
	Sodium bisulfite	14.32	$\$\cdot L^{-1}$	
	Sodium carbonate	44.81	$\$\cdot L^{-1}$	
	Sodium tetraborate	185.93	$\$\cdot kg^{-1}$	
	Water	$0.78 *10^{-3}$	$\$\cdot kg^{-1}$	
	Electricity	0.14	$\$\cdot kWh^{-1}$	
Photocatalytic process	Acetonitrile	5.42	$\$\cdot L^{-1}$	17.05
	Sodium hydroxide	2.19	$\$\cdot kg^{-1}$	
	TiO_2	17.18	$\$\cdot kg^{-1}$	
	Water	$0.78 *10^{-3}$	$\$\cdot kg^{-1}$	
	Electricity	0.14	$\$\cdot kWh^{-1}$	
Hydrothermal catalysis technique	TiO_2	17.18	$\$\cdot kg^{-1}$	2.04
	Water	$0.78 *10^{-3}$	$\$\cdot kg^{-1}$	
	Electricity	0.14	$\$\cdot kWh^{-1}$	
Au value				
1 g Au with 99% purity		75	$\$\cdot g^{-1}$	75

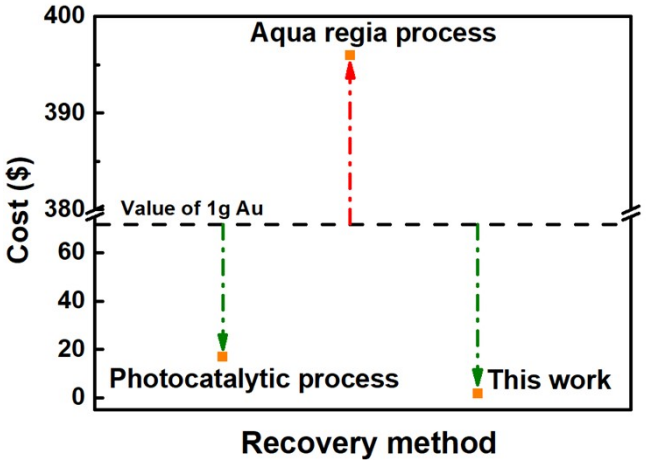

Figure S11 Comparison the cost-benefit of different Au recovery methods.

Table S5 Life cycle inventories of hydrothermal catalysis technique, modeled from our experimental data.

Input	Chemicals	Quantity	Units
Materials	CPUs	1	kg
	TiO_2	$0.8*10^{-3}$	kg
	Water	0.5	kg
Electricity		14.4	kWh
Output	Chemicals	Quantity	Units
	TiO_2	$0.8*10^{-3}$	kg
	Gold	$1*10^{-3}$	kg
	Water	0.5	kg
	Residue	0.989	kg

Table S6 Life cycle inventories of aqua regia process, modeled from the data of ref 1-3.

Input	Chemicals	Quantity	Units
Materials	CPUs	1	kg
	Nitric acid	31.96	kg
	Hydrochloric acid	10.9	kg
	Water	25	kg
	Sodium bisulfite	$0.79*10^{-3}$	kg
	Sodium Carbonate	$1*10^{-4}$	kg
	Sodium tetraborate	$1*10^{-4}$	kg
Electricity		6	kWh
Output	Chemicals	Quantity	Units
	Nitric acid	29.75	kg
	Hydrochloric acid	10.9	kg
	Gold	$1*10^{-3}$	kg
	Sulfuric acid	$0.66*10^{-3}$	kg
	Sodium Carbonate	$1*10^{-4}$	kg
	Sodium tetraborate	$1*10^{-4}$	kg
	Water	25	kg
	Residue	0.97	kg

Table S7 Life cycle inventories of photocatalytic process, modeled from the data of ref 3-4.

Input	Chemicals	Quantity	Units
Materials	CPUs	1	kg
	Acetonitrile	3.66	kg
	Sodium hydroxide	0.05	kg
	TiO_2	$0.5*10^{-3}$	kg
	Water	3.5	kg
Electricity		5.28	kWh
Output	Chemicals	Quantity	Units
	Acetonitrile	2.34	kg
	Sodium hydroxide	0.021	kg
	TiO_2	$0.5*10^{-3}$	kg
	Gold	$1*10^{-3}$	kg
	Water	3.5	kg
	Residue	0.994	kg

References

1. Wang, J., Lu, Y., Xu, Z. Identifying extraction technology of gold from solid waste in terms of environmental friendliness. *ACS Sustainable Chem. Eng.* **7**, 7260-7267 (2019).
2. Liu, Y. Research on the technology of recycling precious metals in waste printed circuit boards in mobile phones. Masters Dissertation. Southwest Jiaotong University, Chengdu, China, 2010 (in Chinese).
3. Shang, H., Chen, Y., Guan, S. *et al.* Scalable and selective gold recovery from end-of-life electronics. *Nat Chem Eng* **1**, 170-179 (2024).
4. Chen, Y. et al. Selective recovery of precious metals through photocatalysis. *Nat. Sustain*. **4**, 618-626 (2021).